



RESEARCH ARTICLE

# Effect of design parameters on strong and immobilizing grasps with an underactuated robotic hand

Roshan Kumar Hota\*  and Cheruvu Siva Kumar 

Mechanical Engineering Department, Indian Institute of Technology, Kharagpur, India

\*Corresponding author. E-mail: roshan1182.iitkgp@gmail.com

Received: 13 June 2021; Revised: 6 March 2022; Accepted: 24 March 2022; First published online: 2 May 2022

**Keywords:** robotic hands, underactuated hands, grasping, mechanism design, immobilizing grasp

## Abstract

This paper presents a study on the effect of design parameters of an underactuated hand on its grasp performance. Three kinds of grasp performance characteristics are considered: grasp range, grasp strength, and immobilizing grasp range. Grasp strength is defined as the stiffness of the grasp. Immobilizing grasps are those in which the object cannot be moved for a force up to a certain threshold. In general, underactuated hands cannot produce immobilizing grasps. However, we show that immobilizing grasps can be created by including joint limits in the hand design. We consider the effect of two design parameters on the grasp performance: torque ratio and finger-base distance. Results show that an optimal finger-base distance and torque ratio exists that maximizes the grasp range and grasp strength. Also, the immobilizing grasp range is increased by decreasing the finger-base distance and increasing the torque ratio and joint limits.

## Nomenclature

$\rho$	Radius ratio or torque ratio
$\tau_i$	Torque produced by the tendon at the $i^{\text{th}}$ joint
$\theta_i$	Joint angle at the $i^{\text{th}}$ joint
$b$	Base length or palm width
$b_r$	Non-dimensionalized base distance ( $= b/r_1$ )
$c_i$	Contact length at the $i^{\text{th}}$ contact
$c_{ir}$	Non-dimensionalized contact length $c_{ir} = c_i/r_1$
$d_x, d_y$	Displacement of the object in the x and y direction, respectively
$f_i$	Contact force at the $i^{\text{th}}$ contact
$f_{a/b/c/d}$	Non-dimensionalized contact forces ( $f_a = f_1/T$ ) and so on
$K_g$	Grasp stiffness matrix
$k_i$	Joint stiffness at the $i^{\text{th}}$ joint
$k_{a/b/c/d}$	Non-dimensionalized joint stiffness ( $k_a = k_1/(Tr_1)$ ) and so on
$l_i$	Link length of the $i^{\text{th}}$ link
$l_{ir}$	Non-dimensionalized link length ( $l_{ir} = l_i/r_1$ )
$O_r$	Non-dimensionalized object radius ( $= r_o/r_1$ )
$Q_k$	Grasp stiffness measure
$r_i$	Radius of the $i^{\text{th}}$ joint pulley
$r_o$	Radius of the object
$T$	Tendon tension
$t$	Distance between line joining joints and contact point (link thickness)

## 1. Introduction

Robotic hands have potential applications in prosthetics, telemanipulation, and service robotics. Robotic hands are mostly being used for grasping tasks with some works focusing on manipulation capabilities. Design of the robot hand depends on the complexity of the grasping or manipulation task. A broad categorization of robot hand design approaches can be based on the actuation scheme or degree of actuation (DOA) – fully actuated and underactuated robotic hands. Fully actuated hands have as many degree of actuation (DOA) as the degree of freedom (DOF) while underactuated hands have fewer actuations than DOF. The choice of the actuation scheme depends on application. Recent trend [1] has been to simplify the design of hand. Underactuation is an important approach for simplified designs.

Underactuated hands require fewer actuators than the degrees of freedom and can be designed to adapt to a wide range of objects. They provide a trade-off between effectiveness and complexity for grasping. The authors in ref. [1] provide an exhaustive list of robotic hands developed since the 1900s. One of the early underactuated hand is the Soft Gripper [2], and some of the recent, notable, underactuated hands are the SDM hand [3], iHY hand [4], Pisa/IIT SoftHand [5], and Velo gripper [6]. These underactuated hands are designed to passively adapt to the shape of the object – a behavior central to the performance of underactuated robotic hands. Therefore, they can grasp a wide array of objects and employ few (in some cases just one [7]) motors. Contrast it with a fully actuated hand like the DLR-Hand II [8] that requires an independent actuator for every degree of freedom making the whole system bulkier, costlier, and difficult to control. Most underactuated hands are designed for enveloping grasp with a few works focusing on fingertip grasps with underactuated hands [9, 10]. The present work focuses on enveloping grasp by underactuated hands.

Although underactuated hands are versatile in enveloping grasp, their precision grasp and manipulation ability is limited. Some works combine active control of fully actuated hand and passive compliance of underactuated hand. The design of an anthropomorphic hand presented by Yang et al. [11] has a fully actuated hand integrated with spring mechanism for passive compliance. Thus, the hand can perform fine manipulation as well as adaptive grasping using the passive compliance.

Underactuated hands use differential mechanisms to resolve one input to two outputs. The differential mechanisms can be implemented using linkages [12] or tendon-pulley systems [13, 14]. Although underactuated hands are simpler, they need to be designed well to be effective. Limitations in their capability should be studied and offset by appropriate design changes. Approaches for underactuated hand design found in literature can be broadly categorized into kinematic design approach and force design approach. The kinematic design approach focuses on the kinematic motion of the fingers without regard to the force application capabilities. Natural closing motion and finger workspace are some of the criteria adopted. Force design approach gives greater importance to force application capabilities of the finger. For example, equal distribution of forces in the finger phalanges or force isotropy [15] is often considered an important criterion.

Robot hands are often designed using basic kinematic analysis and intuition. Some designs include bio-inspiration [16]. There are few works that perform exhaustive parameter space exploration to search for optimal design [17, 18]. In our work, we adopt the force design approach and analyze stability of underactuated fingers in a grasp. Birglen et al. in their book on underactuated hands [19] study underactuated hand mechanisms, kinetostatic analysis, grasp stability of underactuated fingers, and optimal design. In the study, they highlight that there are many configurations in which an underactuated finger cannot grasp an object or cannot create a positive grip. These configurations are called defective and the finger slips on the object in these configurations. It is critical to identify the defective configurations and design the underactuated finger to maximize the stable grasp range. In a stable grasp or positive grip, the contact forces between the fingers and the object are all positive [20, 21]. When one or more contact forces are negative, the grasp becomes defective and the fingers slip on the object. Design of a finger can be improved by increasing the range of stable, positive, grips. Birglen et al. focus on the analysis of single finger. In our work, we analyze the effect of both fingers grasping an object.

Performance of underactuated hands can be quantified and design parameters that maximize the performance can be found [17, 22, 23]. Kragten and Herder [24] analyze stability of grasp by an

underactuated two-fingered hand and define the performance of the hand as its ability to grasp and hold. The ability to grasp means the range of object that the hand can grasp and the ability to hold means the minimum force required to pull an object out of the grasp. They also perform a geometric design optimization [25] to maximize these performance measures. Boisclair et al. [17] adopt a similar approach to optimal design of an underactuated finger based on rolling contact joint. They define performance in terms of uniform distribution of contact forces on the phalanges and the force required to extract the object from the grasp. Ciocarlie and Allen [26] perform formal optimization to maximize a performance measure like the direction and magnitude of the force applied by the hand on the object. A framework for the optimization of the tendon actuation in a biomorphic hand has been presented by Bicchi and Prattichizzo [27]. In our work, we also look at the ability to grasp and find the design parameters that maximize the range of objects grasped by the hand.

Authors in ref. [28] adopt an experimental approach to determine the force application capabilities for different tendon routing. Authors in ref. [29] perform static analysis of the gripper and also check the predicted grasp forces through experiments. However, they do not perform a parametric design exploration or optimization.

Apart from geometric parameters, actuation parameters like joint torque ratio and joint stiffness also play a critical role in determining the performance of a robotic hand. Dollar and Howe [18] perform design exploration of underactuated hands for grasping in an unstructured environment. The key performance measure is the robustness of the grasp against error in position of the object relative to the palm. They test the success and failure of grasp for varying initial positions of the object relative to the palm. They optimize the actuation parameters to improve the grasp performance of the hand. However, they do not propose a notion of strength of grasp.

There has been an effort to extend the notion of form closure to analyze the grasp quality of underactuated hands. Krut et al. [30] highlight that the usual definition of form closure assumes the contact points fixed in space. This is not true for an underactuated hand; thus, the standard form closure definition does not apply to underactuated hands. They propose non-backdrivable actuations for creating form closure with underactuated hands. In our work, we also look at a related concept called immobilizing grasps wherein an object is not displaced by an external forces within a particular threshold. Our work differs as we focus on a design feature, the joint limit, for creating immobilizing grasps. The opposite of the immobilizing grasp is the non-immobilizing grasp that occurs in hands without joint limits. We did not find an extensive study on immobilizing grasps with underactuated hands in the literature.

Based on the literature, we found that study of immobilizing grasps created by non-backdrivable mechanism has been studied [30] but the role of hand design in creating immobilizing grasp has not been carried out. In the present work, we study the role of physical joint limits in creating immobilizing grasps. Although the role of joint limit in stable grasps by a finger has been studied extensively [19], the role they play in creating immobilizing grasps on the object has not been studied well. Kragten et al. [25] introduce immobilizing grasp when they discuss grasps in which the object is pressed against the palm but do not delve into the topics like the role of joint limits. The main contribution of this work is the study of the role of design parameters like the joint limits, base distance, and torque ratio on immobilizing grasps by an underactuated hand. This study has important implications as immobilizing grasps by underactuated hands can be useful to prevent motion of the object due to small external forces.

Apart from immobilizing grasps, we also study the range of objects grasped by the hand and the stiffness of the grasp. The important contributions of this paper are:

- Study on how joint limits can create immobilizing grasps.
- Study on the effect of joint limits on the range of object sizes immobilized.
- Experimental validation of immobilizing grasps.
- Study on the effect of hand design parameters – base distance and torque ratio – on the range of object sizes that are successfully grasped by the hand.

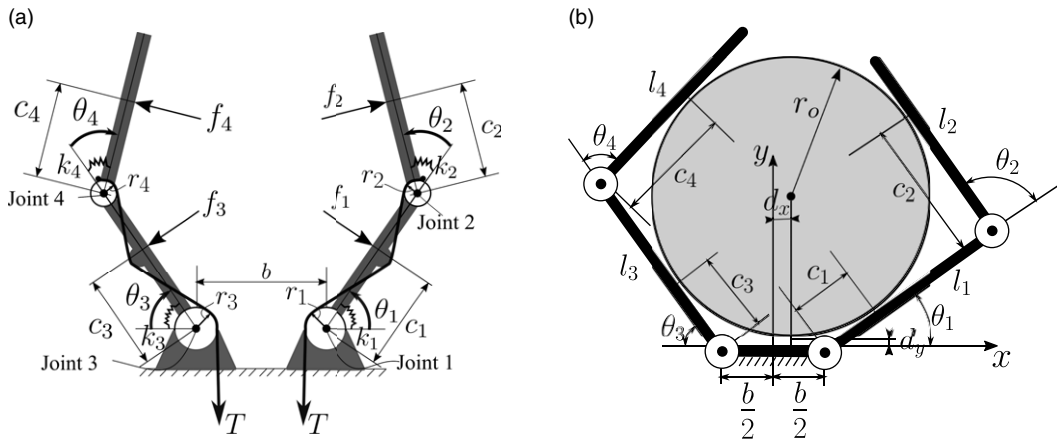


Figure 1. Grasp geometry.

- Study on the effect of hand design parameters, base distance, and torque ratio, on the strength of the grasp defined in terms of grasp stiffness.

## 2. System description

In this work, we study an underactuated, tendon-driven, two-fingered hand shown in Fig. 1(a). For our analysis, the hand grasps an object in the horizontal plane. In this case, the gravity does not act in the plane of the grasp. In the condition when the hand is facing up or down, an external (gravitational) force should be considered on the object. Single tendon runs through both the fingers. Both the fingers are, thus, actuated with tendons having equal tension as shown in Fig. 1(a). Tendons are routed over joint pulleys as shown. The design of hand is similar to the design of SDM hand [3]. The mechanism is a constant torque ratio mechanism. The ratio of the torque created by the tendon at the two joints of a finger is constant (independent of the joint angles).

We assume frictionless contact between the tendon and the joint pulleys or between the fingers and the object. The interaction forces between the finger and object ( $f_1, f_2, f_3, f_4$ ) are therefore perpendicular to the finger surface. The fingers have an active close mechanism – they flex when the tendon is pulled and extend when the tendon is released (due to action of the joint spring). When the fingers are not interacting with an object, the free movement of the finger is governed by the pulley radii and the stiffness of the springs. While Fig. 1(a) shows the two-fingered hand without joint limits, Fig. 5 shows the hand design with joint limits at the proximal joints of the fingers.

A schematic of the hand grasping an object is shown in Fig. 1(b). In this study, we have used a circular object. A circular object simplifies the analysis as it can be specified with one parameter (radius). At the same time, a circular object provides useful insight into the nature of the grasp for objects of different sizes. Thus, we found circular object to be an adequate assumption.

Grasp of the object takes place as follows: hand is positioned near the object with fingers open, fingers start closing and the proximal phalanx makes contact with the object, the finger continues to close and distal phalanx makes contact with the object, the hand pushes the object within the grasp to a position of equilibrium for both the hand and the object.

In certain situations, the grasp may fail due to the fingers slipping on the object. We detect such cases by checking for a feasible equilibrium of hand and object. To analyze this, we develop the grasp model to find the interaction forces between the fingers and the object. Grasp modeling is presented in the following section.

### 3. Grasp modeling

This section presents the procedure for computing the contact forces and the net force on the object. We consider the case of frictionless contact between the fingers and the object. With the frictionless assumption, we perform a worst-case analysis of the underactuated hand. The frictionless case also provides insights into the design features that lead to an unstable grasp.

To compute the contact forces, we consider the object fixed in space at a known position and find the configuration of the hand in contact with the object. Using the configuration of the hand, obtained from geometry, we compute the contact forces required for equilibrium of the fingers. Using the value of the contact forces, applied to the object, we compute the net force on the object.

The reference frame ( $x - y$ ) attached to the palm of the hand is shown in Fig. 1(b). For the position of the object shown, we can use geometry to determine the contact locations ( $c_1, c_2, c_3,$  and  $c_4$ ) and the joint angles ( $\theta_1, \theta_2, \theta_3, \theta_4$ ). For brevity, we do not show the full expressions here.

The expressions for equilibrium of the fingers are Eqs. (1) to (4):

$$\tau_1 = Tr_1 = f_1c_1 + f_2(c_2 + l_1\cos\theta_2) + k_1\theta_1 \tag{1}$$

$$\tau_2 = Tr_2 = f_2c_2 + k_2\theta_2 \tag{2}$$

$$\tau_3 = Tr_3 = f_3c_3 + f_4(c_4 + l_3\cos\theta_4) + k_3\theta_3 \tag{3}$$

$$\tau_4 = Tr_4 = f_4c_4 + k_4\theta_4 \tag{4}$$

In the equations above,  $f_1, f_2, f_3,$  and  $f_4$  are the contact forces on the links 1, 2, 3, and 4 respectively. The torques at the joint ( $\tau_1, \tau_2, \tau_3,$  and  $\tau_4$ ) are produced due to the tension in the tendon ( $T$ ). Torque at the  $i^{th}$  joint produced due to tendon tension is given by:  $\tau_i = Tr_i$ . Here,  $r_i$  is the radius of the  $i^{th}$  joint pulley. From the preceding expression, we find that the joint torque produced due to tendon tension is independent of the configuration of the finger. The angular stiffness of the springs at the joints are  $k_1, k_2, k_3,$  and  $k_4$ .

The next step in modeling of the system is to non-dimensionalize the preceding expressions. We divide Eqs. (1), (2), (3), and (4) by the term  $Tr_1$  to obtain the following expressions (Eqs. (5) to (8)):

$$1 = \frac{f_1}{T} \frac{c_1}{r_1} + \frac{f_2}{T} \left( \frac{c_2}{c_1} + \frac{l_1}{c_1} \cos\theta_2 + \frac{k_1}{Tr_1} \theta_1 \right) \tag{5}$$

$$\frac{r_2}{r_1} = \frac{f_2}{T} \frac{c_2}{r_1} + \frac{k_2}{Tr_1} \theta_2 \tag{6}$$

$$1 = f_a c_{1r} + f_b (c_{2r} + l_{1r} \cos\theta_2) + k_a \theta_1 \tag{7}$$

$$\rho = f_b c_{2r} + k_b \theta_2 \tag{8}$$

where

$$\rho = \frac{r_2}{r_1}, f_a = \frac{f_1}{T}, f_b = \frac{f_2}{T}, c_{1r} = \frac{c_1}{r_1}, c_{2r} = \frac{c_2}{r_1}, l_{1r} = \frac{l_1}{r_1}, k_a = \frac{k_1}{Tr_1}, k_b = \frac{k_2}{Tr_1}$$

In the expressions above, forces are non-dimensionalized by division of the tendon tension ( $T$ ), all lengths are non-dimensionalized by the proximal joint radius  $r_1$ , and the stiffnesses are non-dimensionalized by the product  $Tr_1$ .

Rearranging to find the non-dimensionalized forces  $f_a$  (Eq. (9)) and  $f_b$  (Eq. (10)).

$$f_a = \frac{1}{c_{1r}} \left[ 1 - k_a \theta_1 - (\rho - k_b \theta_2) \left( 1 + \frac{l_{1r}}{c_{2r}} \cos\theta_2 \right) \right] \tag{9}$$

And,

$$f_b = \frac{1}{c_{2r}}(\rho - k_b\theta_2) \quad (10)$$

Similarly, the expressions of the contact forces for the other finger,  $f_c$  (Eq. (11)) and  $f_d$  (Eq. (12)) can be calculated as:

$$f_c = \frac{1}{c_{3r}} \left[ 1 - k_c\theta_3 - (\rho - k_d\theta_4) \left( 1 + \frac{l_{3r}}{c_{4r}} \cos\theta_4 \right) \right] \quad (11)$$

And,

$$f_d = \frac{1}{c_{4r}}(\rho - k_d\theta_4) \quad (12)$$

The non-dimensionalized object radius is given by  $O_r = r_o/r_1$ , and the non-dimensionalized base distance is given by  $b_r = b/r_1$ . Radius ratio ( $\rho = r_2/r_1$ ) is an important design parameter which is equal to the inter-phalangeal torque ratio (Eq. (13)).

$$\frac{\tau_2}{\tau_1} = \frac{r_2}{r_1} \quad (13)$$

In our analysis, we take the radius ratio/ torque ratio of the left and right finger to be equal. Hence, the radius ratio is given by Eq. (14)

$$\rho = \frac{r_2}{r_1} = \frac{r_4}{r_3} \quad (14)$$

The analysis presented in this paper is for the non-dimensionalized parameters  $O_r$ ,  $\rho$ , and  $b_r$ . For example, we have presented the result for  $O_r = 10.0$ ,  $\rho = 1.0$ , and  $b_r = 6.0$ . Since these parameters are non-dimensionalized with respect to the radius of the proximal joint pulley  $r_1$ , we can obtain the actual dimensions of the parameters by first choosing  $r_1$ . The choice of  $r_1$  will be based on physical constraint on its dimensions. For example, we might choose  $r_1 = 5.0$  mm; then, the base distance we are working with becomes  $b = b_r r_1 = 30.0$  mm, the object size becomes  $r_o = O_r r_1 = 50.0$  mm, and the radius of the distal joint pulley becomes  $r_2 = r_1 \rho = 5.0$  mm.

If we have a tendon tension  $T = 5.0$  N, then the torque at both the joints is  $\tau_i = T r_1 = 25.0$  Nmm,  $i = 1, 2, 3, 4$ . The joint angles for an equilibrium position of hand and object are  $\theta_1 = 0.39$  rad,  $\theta_2 = 1.61$  rad,  $\theta_3 = 0.39$  rad, and  $\theta_4 = 1.61$  rad. And the corresponding contact forces are  $f_1 = f_3 = 0.206$  N and  $f_2 = f_4 = 0.457$  N. And the non-dimensionalized forces are  $f_a = f_c = f_1/T = 0.0412$  and  $f_b = f_d = f_2/T = 0.0914$ .

Since the goal of this study is to evaluate the success of a hand design to grasp objects, detection of successful and defective grasps through simulation is critical. We do this by searching for a feasible equilibrium of the hand and object. If a feasible equilibrium of both hand and object is found, the grasp is successful else it is defective. Defective grasp physically means that the fingers will slip on the object and grasp will fail. The process of detecting grasp success and failure cases is called grasp analysis.

As explained earlier, to ascertain whether a grasp is successful, we “search” for a feasible equilibrium position of both the hand and the object. For this, we fix the object at different locations relative to the palm and determine the net force on the object applied by the hand. If the net force is zero, we have found the equilibrium position. If not, we iterate the process with a new candidate location of the object. This process when applied to hand designs with joint limits has to first eliminate the location of the object where the joint limits of the fingers will be violated.

In the following section, we describe, in detail, the various conditions that has been taken into account to detect grasp success and failure.

#### 4. Grasp analysis

In grasp analysis, we computationally determine the success and failure of grasps. We also determine the strength of the grasp using the grasp stiffness measure. We consider four- and five-point grasps. A

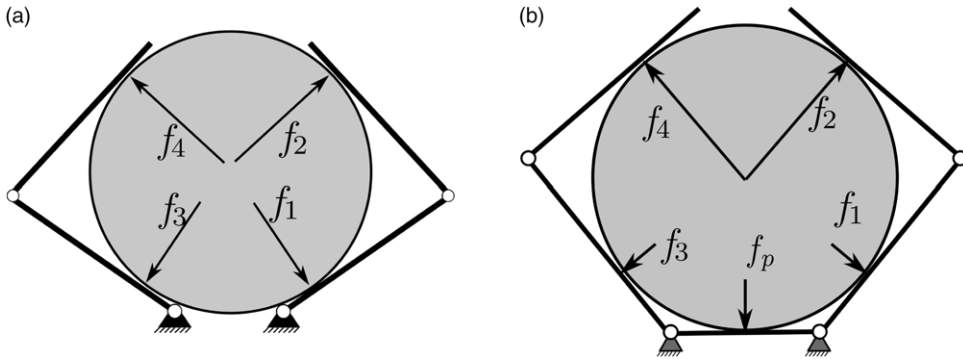


**Figure 2.** Two cases of successful grasp by the hand (a) having four contacts only with the fingers (b) having five contacts, four with the fingers and one with the palm.

five-point grasp is one in which the object touches the palm of the hand. In a four-point grasp, contact takes place only with the fingers. The steps involved in determining the success and failure of the grasp are as follows:

1. Locate the object at a position relative to the palm. The object is considered fixed at this location, and we determine the force exerted by the underactuated hand on the object.
2. From geometry, determine the contact locations and joint angles for the fingers to contact the object (Fig. 1(b)).
3. Determine the forces required for the equilibrium of the fingers in the computed configuration.
4. Check if all the contact forces are positive. If any contact force is negative, the position is not a feasible position of the object and a new position needs to be considered.
5. If all the contact forces are positive, compute the net force on the object applied by the fingers.
6. If the net force is zero, an equilibrium has been found. If the net force is not zero, then the present position is not the equilibrium position of the hand-object system and a new position of the object should be considered.
7. Iterate the process till an equilibrium is found. If equilibrium is not found for bounded candidate positions of the object, the object is not graspable by the hand.

Using the steps given above, we can determine whether an object is graspable by hand. The algorithm for determining success and failure of grasp was implemented in MATLAB. Figure 2 shows two cases of successful grasps with the object having contact only with the fingers (Fig. 2(a)) and having contact with the fingers and the palm (Fig. 2(b)). The range of object sizes that the hand can grasp is one of the performance measures we consider in this work. If the object is graspable, we can define the stiffness of the grasp as detailed in the following section.

#### 4.1. Grasp stiffness

When a grasped object is perturbed from its position, the hand passively applies a restoring force on the object to bring it back to its equilibrium position. The matrix  $K_g$  maps the perturbation to the restoring force (Eq. (15)). The form of the grasp stiffness matrix is shown in Eq. (16). We define the grasp stiffness performance measure ( $Q_x$ ) as the determinant of the grasp stiffness matrix (Eq. (17)).

$$\begin{bmatrix} \Delta F_x \\ \Delta F_y \end{bmatrix} = K_g \begin{bmatrix} \Delta x \\ \Delta y \end{bmatrix} \tag{15}$$

$$K_g = \begin{bmatrix} \frac{\Delta F_x}{\Delta x} & \frac{\Delta F_x}{\Delta y} \\ \frac{\Delta F_y}{\Delta x} & \frac{\Delta F_y}{\Delta y} \end{bmatrix} \quad (16)$$

$$Q_k = |K_g| \quad (17)$$

## 4.2. Immobilizing grasps

Additional conditions should be checked to determine if the object is in immobilizing grasp. First, the joint angle limit should be reached. This implies that the physical joint stops prevent further motion of the fingers. Second, the net force on the object in this condition should be towards the palm. If the net force is away from the palm, the object will be pushed out of the grasp. This usually happens for large objects. When a successful grasp takes place and joint limits are reached, an immobilizing grasp takes place. This implies that a force up to a certain limit is required before the object can be moved. The intuition is that when the object is pulled by the external force, the reaction force provided by the joint limits first go to zero and an additional force moves the object. This also implies that if the tendon tension is increased, external force required to pull the object out of the grasp will also increase. Contrast this with the non-immobilizing grasp where increasing the tendon tension does not make the object immobile.

## 5. Results and discussions

In this section, we present the result for the two categories of hand designs that we analyze in this work – with and without joint limits.

For hand designs without joint limits, we study the effect of torque ratio ( $\rho$ ) and base distance ( $b_r$ ) on the largest object that can be grasped by the hand which is an important performance criterion for underactuated hands. We also show the effect of object size ( $O_r$ ) and torque ratio ( $\rho$ ) on grasp strength quantified in terms of the grasp stiffness.

For hand designs with joint limits, we study the effect of base distance, value of joint limits, and torque ratio on the range of object size that is immobilized. We also show that objects are immobilized in both x and y direction by unequal joint limits for the left and right fingers. Joint limits are enforced using physical stops – physical features in the palm or the finger itself that prevent rotation of the fingers after a certain angle. For example, Fig. 5 shows the joint limit in the form of a feature protruding out of the (extended) palm preventing the rotation of the fingers.

### 5.1. Effect of design parameters on the largest object size grasped

This result is presented for hand designs without joint limits. Figure 3 shows the variation of the largest object grasped ( $\max(O_r)$ ) with the torque ratio ( $\rho$ ) and the base distance ( $b_r$ ). The result shows that  $\max(O_r)$  is largest for a small torque ratio ( $\rho$ ) of around 0.5. For this  $\rho$ , the normalized base distance that maximizes  $\max(O_r)$  is in the range eight to twelve. We also find that for every  $\rho$  there is a range of base distance that maximizes  $\max(O_r)$ . The result is presented for all the combinations of values given in Table I. The step sizes of the three variables ( $O_r$ ,  $b_r$ , and  $\rho$ ) used in the analysis are chosen based on two criteria: to get sufficiently detailed parameter space results and to limit the computation time. The step size of  $b_r$  is chosen to be larger because our initial analysis showed that the effect of this parameter is distinct over a larger range.

The torque ratio has two kinds of effects on the grasp: having a small torque ratio tends to push the object out of the grasp and having a large torque ratio leads to unstable finger configuration wherein



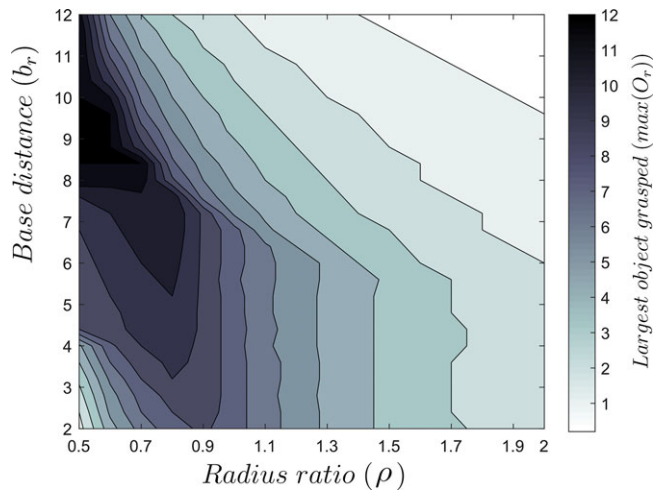


**Figure 3.** Variation of the largest object grasp ( $\max(O_r)$ ) with the torque ratio ( $\rho$ ) and the base distance ( $b_r$ ).

the finger slips on the object and grasp ejection takes place. Hence, in Fig. 3 we find that for  $b_r = 6$ , for example, largest grasp range is obtained for  $\rho$  of around 0.8. The grasp range decreases both by increasing and decreasing the torque ratio.

### 5.2. Effect of design parameters on grasp stiffness

Grasp stiffness measures the restoring force that the hand applies on the object for its small displacement within the grasp. We use this measure for quantifying the strength of the grasp. The determinant of the grasp stiffness matrix ( $K_g$ ) is a measure of the grasp stiffness ( $Q_k$ ). Here, we present the effects of object size and torque ratio on grasp stiffness. Figure 4 shows the variation of grasp stiffness ( $Q_k$ ) with radius ( $\rho$ ) for different object sizes. From the results, we observe that for every object size there is an optimal torque ratio that maximizes the grasp stiffness. Further, the optimal  $\rho$  is, in general, larger for smaller objects. This is not something we would expect. A larger torque ratio means that the torque at the distal joint is larger than the proximal joint. This should lead to more force towards the palm of the hand. However, we find an optimal torque ratio ( $\rho$ ). This result is useful for designing underactuated hands for specific objects. The mechanism we have used is a constant torque ratio mechanism. We can consider a mechanism with configuration-dependent torque ratio, and it can be designed such that the torque ratio increases as the finger flexes. This will lead to a better design for objects of varying sizes.

### 5.3. Joint limits can help create immobilizing grasps

In this section, we study the effect of joint limits in creating immobilizing grasps with underactuated hands. Objects grasped with underactuated hands can be moved with an external force due to their inherent compliance. Thus, the grasps are, in general, non-immobilizing. However, joint limits can help create immobilizing grasps – the object cannot be moved for external force up to a certain limit. Introducing joint limits can create immobilizing grasps because the final grasp condition is such that the fingers of the hand apply a net force on the object. In order to move the object, this force has to be first overcome by the external force.

Figure 5 shows the final position of the object with (black lines) and without (faded red lines) joint limits. The idea is to use physical joint limits to restrict the object at a location where the fingers apply a net force on the object. This implies that an equal external force should be exceeded before the object

**Table I.** Parameters and their values used for computation.

Parameter	Range	Step
$O_r$	[4,12]	0.2
$b_r$	[2,14]	1
$\rho$	[0.5,2.0]	0.1

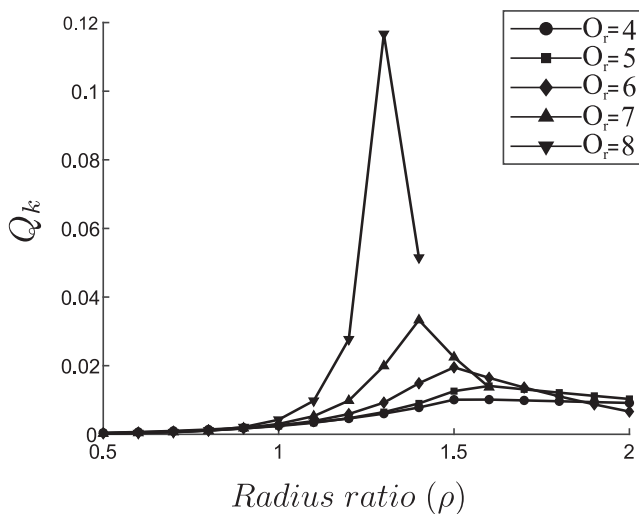


**Figure 4.** Variation of grasp stiffness ( $Q_k$ ) with torque ratio ( $\rho$ ) for different object sizes ( $O_r$ ). The computation has been performed for  $b_r = 9$ .

moves. Without joint limits, at the final position of the object within the grasp, the net force applied by the fingers on the object is zero and the object can be moved within the grasp even for a small external force. This happens due to the inherent compliance of the underactuated hand mechanism. The joint limit, as shown in Fig. 5, is used at the proximal joints of both fingers. With equal joint limits in the left and right fingers, the object is made immobile in only y-direction. By using unequal joint limits for the left and right fingers, an object can be made immobile in both x and y directions. This is because with unequal joint limits, a net force is applied, by the fingers, on the object in both x and y directions whereas for equal joint limits, the net force is applied only in the y-direction.

**5.4. Effect of design parameters on the range of object size immobilized**

In this section, we investigate how the hand design parameters – joint limit, torque ratio, and base distance – affect the range of object sizes that are immobilized. Important conclusions from the result are as follows:

1. Increasing joint limits increases the range of object size immobilized.
2. Increasing base distance decreases the range of object size immobilized.
3. Increasing the torque ratio, in general, increases the range of object size immobilized.

These results point to the underlying phenomena that the range of object size immobilized is larger if the joint limits can come into play more easily. Figure 6(a) shows the variation of the range of object size ( $O_r$ ) immobilized with the torque ratio ( $\rho$ ). We observe that the range of object size immobilized is

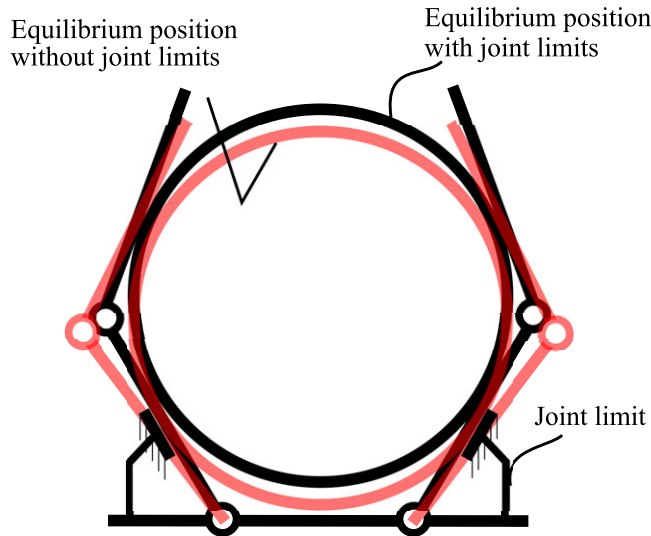


**Figure 5.** Illustration of final position of the object with (black lines) and without (faded red lines) joint limits.

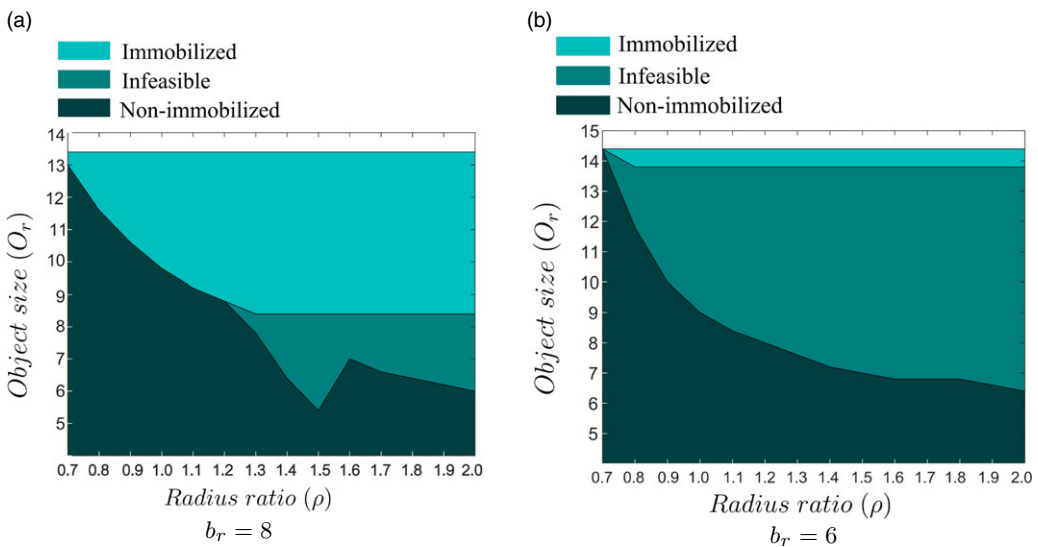


**Figure 6.** Variation of the range of object size ( $O_r$ ) immobilized with torque ratio ( $\rho$ ) for different  $b_r$ 's ( $\theta_{lim} = 0.40$  rad and  $\theta_{3lim} = 0.35$  rad).

very small in this case. The joint limits, in this case, are  $\theta_{lim} = 0.40$  rad and  $\theta_{3lim} = 0.35$  rad for the left and right proximal joints, respectively. If we decrease the base distance, keeping the joint limits same, we can obtain a larger range of object sizes that are immobilized. Figures 6(b) and 7(a) show the result for  $b_r = 6$  and  $b_r = 4$ , respectively.

Figure 7(b) shows the range of object sizes immobilized for larger joint limits ( $\theta_{lim} = 0.60$  rad and  $\theta_{3lim} = 0.55$  rad). Contrast this with the result presented in Fig. 6(b) for the same  $b_r$ . We note that the range of object size immobilized increases by increasing the joint limit. However, we should also note that the largest size immobilized decreases on increasing the joint limits.

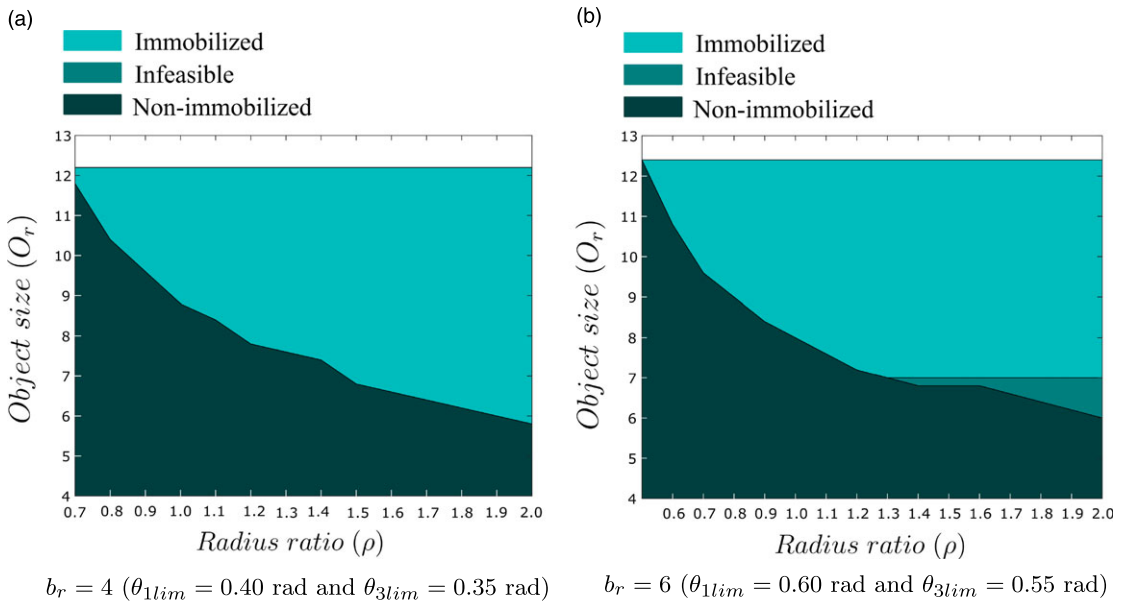


**Figure 7.** Variation of the range of object size ( $O_r$ ) immobilized with torque ratio ( $\rho$ ) for different  $b_r$ 's and joint limits.

### 5.5. Simulation verification of the results

To verify some of our results, we conducted simulations with MATLAB's Simscape Multibody software. We model contact force between hand and object using the Spatial Contact Force block. We verified our contact force model using the contact force sensing feature in the software.

We conducted simulation of scenarios with and without joint limits and present the results in following sections.

#### 5.5.1. Simulation of grasping by hand designs not having joint limits

We conducted simulation with different base distance and torque ratio to verify our results. These simulations are for hand designs without joint limits. Here we show in a tabular form the correspondence between simulation result and computation result as a function of the object sizes that can be grasped. Table II shows the correspondence between simulation and computation results for three sample cases. The results show that for  $b_r = 6.0$  and  $\rho = 1.0$ , object of size  $O_r = 10.0$  can be grasped while object of size  $O_r = 12.0$  cannot be grasped. Also, by reducing  $\rho$  to 0.7, object with radius  $O_r = 12.0$  can be grasped. We obtained the same results with our computation model as well. The grasp sequence of a successful and a failure case is shown in Figs. 8 and 9, respectively.

#### 5.5.2. Simulation of immobilizing grasps

We perform the simulation verification of our results using MATLAB's Simscape Multibody library. To simulate immobilizing grasps, we introduce joint limits. Joint limits can be directly included in the revolute joint block of Simscape Multibody. We apply external force to the object to see its affect on object position. We consider two cases here, two different object sizes, one that is immobilized and one that is not immobilized.

**Table II.** Comparison between simulation and computation for two cases without joint limits.

$b_r$	$\rho$	$O_r$	Computation	Simulation
6.0	1.0	10.0	Success	Success
6.0	1.0	12.0	Failure	Failure
6.0	0.7	12.0	Success	Success

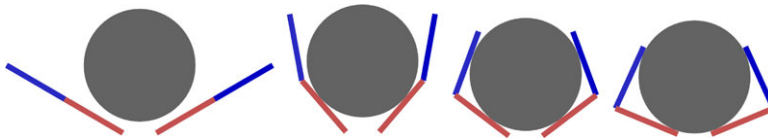


**Figure 8.** Grasp sequence for a successful grasp with  $\rho = 1.0$ ,  $b_r = 6.0$ , and  $O_r = 10.0$ . There are no joint limits.

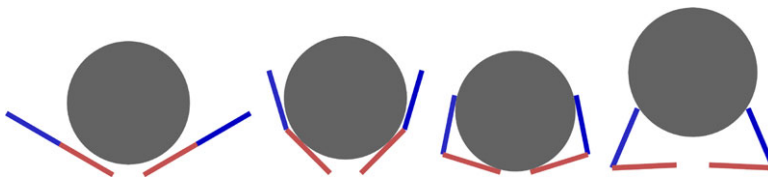


**Figure 9.** Grasp sequence for a failed grasp with  $\rho = 1.0$ ,  $b_r = 6.0$ , and  $O_r = 12.0$ . There are no joint limits.

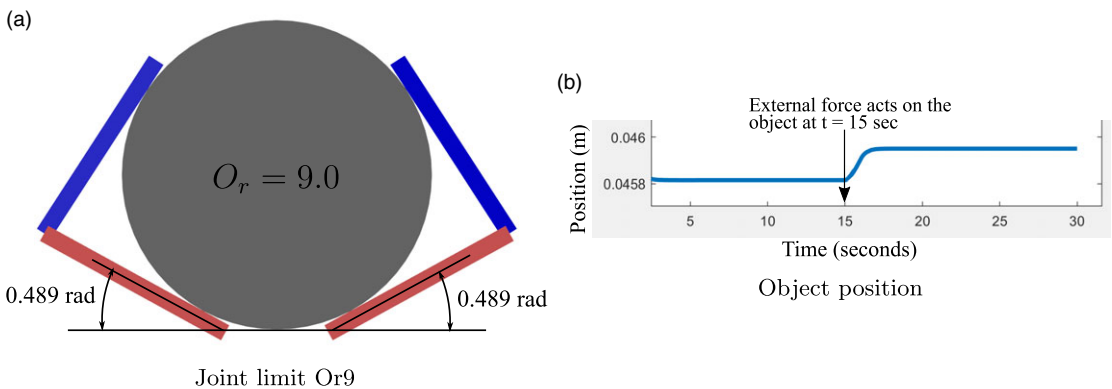


**Figure 10.** Grasp simulation using MATLAB Simscape Multibody: (a) object ( $O_r = 9.0$ ) not immobilized by the hand ( $\rho = 1.0$  and  $b_r = 6.0$ ), (b) object is displaced when an external force acts on the object ( $t = 15$  s).

The object size used are  $O_r = 9.0$  and  $O_r = 12.0$ . The hand design is as follows:  $b_r = 6.0$ ,  $\rho = 1.0$ , joint limit at the proximal joint of right finger is 0.35 rad and joint limit on the proximal joint of left finger is 0.45 rad. Object with size  $O_r = 9.0$  is not immobilized. In Fig. 10(a), we see that the joint limit is not reached, joint angle is 0.489 rad. Therefore, the object is not held in an immobilizing grasp. If an external force acts on the object, the object will displace from its position. Figure 10(b) shows the displacement of the object due to a small force that acts on the object at  $t = 15$  sec.

Object with size  $O_r = 12.0$  is held in an immobilizing grasp by the same hand. An external force acting on the object will not displace the object. Figure 11(a) shows that the joint limits are reached.

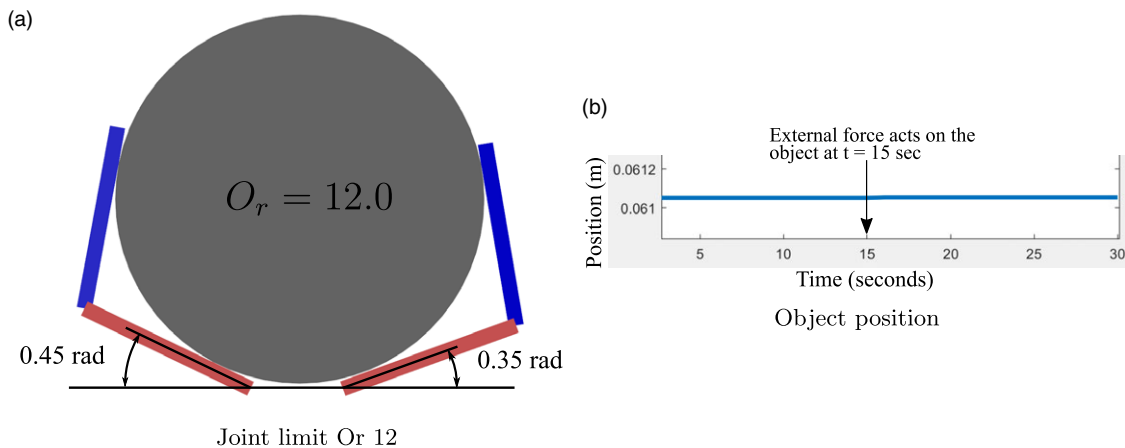


**Figure 11.** Grasp simulation using MATLAB Simscape Multibody: (a) Object ( $O_r = 12.0$ ) immobilized by the hand ( $\rho = 1.0$  and  $b_r = 6.0$ ), (b) object is not displaced when an external force acts on the object at  $t = 15$  s.

Figure 11(b) shows that the object is not displaced by the small force acting on it. These simulation results show the effectiveness of joint limits in creating immobilizing grasps.

### 6. Experimental validation

In this section, we perform experimental validation for immobilizing grasps. We compare the immobilizing grasps found in simulation to that in the experiment. For experiments, we have made the two-fingered underactuated hand with 3D printing. Table III shows the comparison between simulation (MATLAB Simscape Multibody) and experimental results. The comparison is performed for two object sizes and two radius ratios ( $\rho = 1.0$  and  $\rho = 1.5$ ). Absolute values of the parameters used for verifying the results is shown in Table IV.

In the results presented in Table III, we validate our work with the match between the experimental results and simulation results. In the experimental results, immobilizing grasp is one in which joint limits are reached. In such a grasp, tendon tension can be increased to resist larger external forces on the object. Figures 12(a) and (b) show the grasps with hands made with the parameters from Table IV.

The experimental result also shows the same trend presented in Fig. 7. The major trends are as follows:

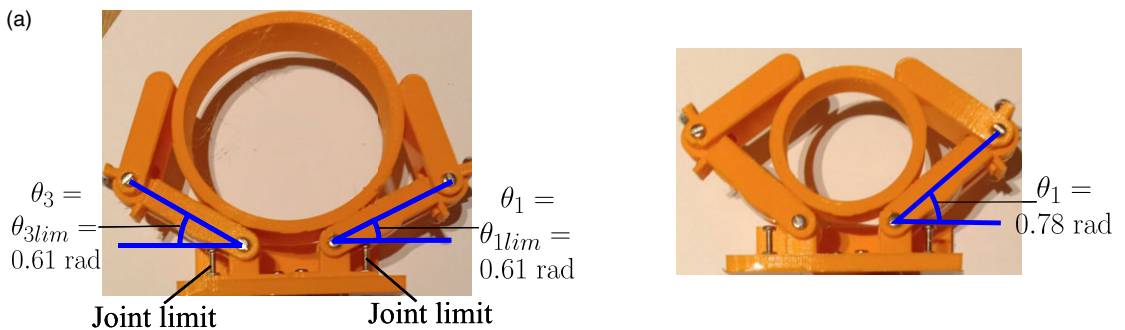
- Larger objects are immobilized: We see this in case of both  $\rho = 1.0$  and  $\rho = 1.5$ . The larger object ( $r_o = 40$  mm or  $O_r = 10.0$ ) is immobilized while the smaller object ( $r_o = 25$  mm or  $O_r = 6.25$ ) is not immobilized.
- Using larger torque ratio increases the chances of achieving an immobilizing grasp: If we compare the grasps by hand design with  $\rho = 1.5$  and  $\rho = 1.0$  on the smaller object ( $r_o = 25$  mm or  $O_r = 6.25$ ) (Table III number 2 and 4), we observe that the equilibrium angle for  $\rho = 1.5$  is smaller. This implies that we can create an immobilizing grasp with smaller joint limit angle for a hand having a larger torque ratio.
- Larger joint limits lead to larger range of objects immobilized: This is evident from the result for smaller objects. Consider  $O_r = 6.25$  and  $\rho = 1.5$  (Table III number 4). Since the equilibrium of the object is reached at  $\theta_1 = \theta_2 = 0.87$  rad, a joint limit angle larger than this will create immobilizing grasp on the object. However, we should also note that the size of the largest object grasp also decreases with increase in the joint limit angle.

**Table III.** Comparison of simulation and experimental results ( $l_r = 11.25$  (45 mm)). I: Immobilized, NI: Not immobilized.

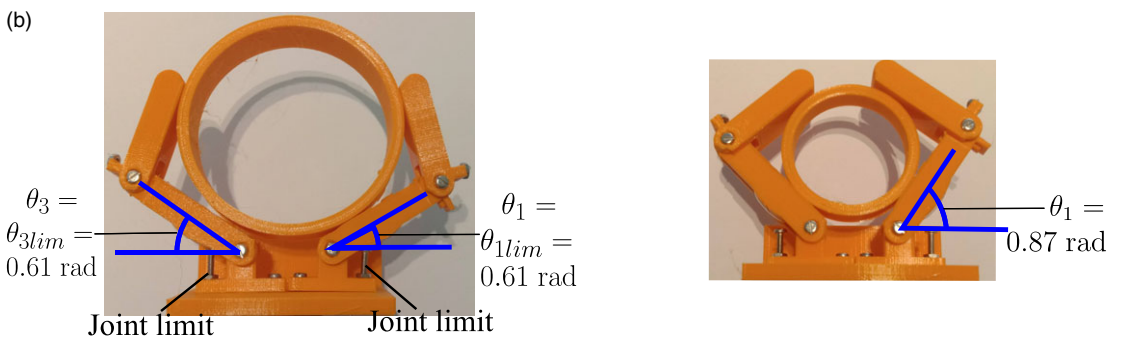
S. No.	$b_r$	$\rho$	$\theta_{1lim} = \theta_{3lim}$	$\theta_1 = \theta_2$	$O_r$	Sim	Exp
1.	7.5	1.5	0.61 rad	0.61 rad	10.00	I	I
2.	7.5	1.5	0.61 rad	0.78 rad	6.25	NI	NI
3.	7.5	1.0	0.61 rad	0.61 rad	10.00	I	I
4.	7.5	1.0	0.61 rad	0.87 rad	6.25	NI	NI

**Table IV.** Values of the parameters used for experimental results.

Parameter	Value
$r_1$	4 mm
$r_2$	{ 4 mm, 6 mm }
$r_o$	{ 25 mm, 40 mm }
$b$	30 mm
$l_1$	45 mm
$\theta_{lim}$ and $\theta_{3lim}$	0.61 rad



Grasp with  $\rho = 1.5$ . (Left)  $O_r = 10.00$  (Table III), S.No. 1), joint-limits are reached and the object is immobilized. (Right)  $O_r = 6.25$  (Table III), S.No. 2), joint-limits are not reached and the object is not immobilized.



Grasp with  $\rho = 1.0$ . (Left)  $O_r = 10.00$  (Table III), S.No. 3), joint-limits are reached and the object is immobilized. (Right)  $O_r = 6.25$ , (Right)  $O_r = 6.25$  (Table III), S.No. 4), joint-limits are not reached and the object is not immobilized.

**Figure 12.** Experimental verification of results.

## 7. Conclusion

In this paper, we studied the effect of design parameters of an underactuated hand on the following performance criterion: ability to grasp a range of objects, grasp strength, and ability to create immobilizing grasps. A key contribution of this work is the study of effect of design parameters on immobilizing grasps. We have presented theoretical, simulation, and experimental results. We have used a disc-shaped object to test the performance of the hand and neglected friction as a conservative assumption. Varying the radius of the disc gives objects of different sizes. The design parameters include the base distance between the two fingers (palm size), torque ratio or radius ratio between the joint pulleys, and the joint limit angle.

We plot the variation of the three performance criterion with the design parameters of the hand. Based on the results, we draw the following conclusions:

1. There is an optimal base distance and torque ratio combination that maximizes the size of the largest object grasped by the hand. This result indicates that optimal values of base distance and radius can be found to obtain the hand design with best grasp performance.
2. We observed that, for every object size, an optimal torque ratio exists that maximizes the strength of the grasp. If for an application the size of the object is known beforehand, an optimum torque ratio can be obtained to maximize grasp strength. Also, this result opens up the possibility of a variable torque ratio mechanism that can grasp objects of different sizes.
3. Immobilizing grasps can be important in many applications. Underactuated hands usually do not create immobilizing grasps. They can create immobilizing grasps when the object, in the final equilibrium position, is in contact with the palm of the hand. This creates immobilizing grasp in the direction perpendicular to the palm. A grasp can be made immobile both perpendicular to and along the palm by introducing joint stops or physical joint limits at the proximal joints of both fingers. The joint limit angle should be different in the left and right fingers.
4. The range of object size immobilized can be increased by increasing the joint limits, decreasing the base distance, and increasing the torque ratio. However, this also leads to a decrease in the size of the largest object immobilized.

**Author contributions.** Roshan Kumar Hota and Cheruvu Siva Kumar conceived and designed the work. Roshan Kumar Hota performed the simulations and generation of results.

**Financial support.** This research received no specific grant from any funding agency, commercial or not-for-profit sectors.

**Competing interests declaration.** The authors have no competing interests to declare.

## References

- [1] C. Piazza, G. Grioli, M. G. Catalano and A. Bicchi, "A century of robotic hands," *Annu. Rev. Control Robot. Auton. Syst.* **2**(1), 1–32 (2019).
- [2] S. Hirose and Y. Umetani, "The development of soft gripper for the versatile robot hand," *Mech. Mach. Theory* **13**(3), 351–359 (1978).
- [3] A. M. Dollar and R. D. Howe, "A highly adaptive SDM hand: Design and performance evaluation," *Int. J. Robot. Res.* **5**(5), 585–597 (2010).
- [4] L. U. Odhner, L. P. Jentoft, M. R. Claffee, N. Corson, Y. Tenzer, R. R. Ma, M. Buehler, R. Kohout, R. D. Howe and A. M. Dollar, "A compliant, underactuated hand for robust manipulation," *Int. J. Robot. Res.* **33**(5), 736–752 (2014).
- [5] M. G. Catalano, G. Grioli, E. Farnioli, A. Serio, C. Piazza and A. Bicchi, "Adaptive synergies for the design and control of the Pisa/IIT softHand," *Int. J. Robot. Res.* **33**(5), 768–782 (2014).
- [6] M. Ciocarlie, F. M. Hicks, R. Holmberg, J. Hawke, M. Schlicht, J. Gee, S. Stanford and R. Bahadur, "The Velo gripper: A versatile single-actuator design for enveloping, parallel and fingertip grasps," *Int. J. Robot. Res.* **33**(5), 753–767 (2014).
- [7] C. Gosselin, F. Pelletier and T. Laliberte, "An Anthropomorphic Underactuated Robotic Hand with 15 DoFs and A Single Actuator," *In: 2008 IEEE International Conference on Robotics and Automation (ICRA)* (2008) pp. 749–754.



- [8] J. Butterfaß, M. Grebenstein, H. Liu and G. Hirzinger, “DLR-Hand II: Next Generation of a Dextrous Robot Hand,” *In: IEEE International Conference on Robotics and Automation (ICRA)*, 2001, vol. 1 (2001) pp. 109–114.
- [9] R. K. Hota and C. S. Kumar, “Effect of hand design and object size on the workspace of three-fingered hands,” *Mech. Mach. Theory* **133**(14), 311–328 (2019).
- [10] G. A. Kragten, M. Baril, C. Gosselin and J. L. Herder, “Stable precision grasps by underactuated grippers,” *IEEE Trans. Robot.* **27**(6), 1056–1066 (2011).
- [11] H. Yang, G. Wei, L. Ren, Z. Qian, K. Wang, H. Xiu and W. Liang, “A low-cost linkage-spring-tendon-integrated compliant anthropomorphic robotic hand: MCR-Hand III,” *Mech. Mach. Theory* **158**, 104210 (2021).
- [12] D. Wang, Y. Xiong, B. Zi, S. Qian, Z. Wang and W. Zhu, “Design, analysis and experiment of a passively adaptive underactuated robotic hand with linkage-slider and rack-pinion mechanisms,” *Mech. Mach. Theory* **155**(2), 104092 (2021).
- [13] C. Rossi, S. Savino, V. Niola and S. Troncone, “A study of a robotic hand with tendon driven fingers,” *Robotica* **33**(5), 1034–1048 (2015).
- [14] V. Babin and C. Gosselin, “Mechanisms for robotic grasping and manipulation,” *Annu. Rev. Control Robot. Auton. Syst.* **4**(1), 573–593 (2021).
- [15] S. Krut, “A Force-Isotropic Underactuated Finger,” *In: IEEE International Conference on Robotics and Automation (ICRA)*, 2314–2319 (2005).
- [16] M. Su, Y. Guan, D. Huang and H. Zhu, “Modeling and analysis of an adaptive soft gripper with the bio-inspired compliant mechanism,” *Bioinspir. Biomim.* **16**(5), 055001 (2021).
- [17] J. M. Boisclair, T. Laliberté and C. Gosselin, “On the optimal design of underactuated fingers using rolling contact joints,” *IEEE Robot. Automat. Lett.* **6**(3), 4656–4663 (2021).
- [18] A. M. Dollar and R. D. Howe, “Joint coupling design of underactuated hands for unstructured environments,” *Int. J. Robot. Res.* **30**(9), 1157–1169 (2001).
- [19] L. Birglen, T. Laliberté and C. M. Gosselin, *Underactuated Robotic Hands*, vol. 40 (Springer, Berlin, Heidelberg, 2007).
- [20] L. Birglen and C. M. Gosselin, “On the Force Capability of Underactuated Fingers,” *In: 2003 IEEE International Conference on Robotics and Automation (ICRA)*, vol. 1 (2003) pp. 1139–1145.
- [21] L. Birglen and C. M. Gosselin, “Kinetostatic analysis of underactuated fingers,” *IEEE Trans. Robot. Autom.* **20**(2), 211–221 (2004).
- [22] M. Ciocarlie and P. Allen, “A Design and Analysis Tool for Underactuated Compliant Hands,” *In: 2009 IEEE/RSJ International Conference on Intelligent Robots and Systems (ICRA)* (2009) pp. 5234–5239.
- [23] G. Li, P. Xu, S. Qiao and B. Li, “Stability analysis and optimal enveloping grasp planning of a deployable robotic hand,” *Mech. Mach. Theory* **158**, 104241 (2021).
- [24] A. G. Kragten and J. L. Herder, “The ability of underactuated hands to grasp and hold objects,” *Mech. Mach. Theory* **45**(3), 408–425 (2010).
- [25] G. A. Kragten, F. C. T. V. Helm and J. L. Herder, “A planar geometric design approach for a large grasp range in underactuated hands,” *Mech. Mach. Theory* **46**(8), 1121–1136 (2011).
- [26] M. Ciocarlie and P. Allen, “A constrained optimization framework for compliant underactuated grasping,” *Mech. Sci.* **2**(1), 17–26 (2011).
- [27] A. Bicchi and D. Prattichizzo, “Analysis and optimization of tendinous actuation for biomorphically designed robotic systems,” *Robotica* **18**(1), 23–31 (2000).
- [28] A. B. Clark, L. Liow and N. Rojas, “Force evaluation of tendon routing for underactuated grasping,” *J. Mech. Design* **143**(10), 104502 (2021).
- [29] A. C. A. R. Osman, H. Sağlam and Ş. A. K. A. Ziya, “Evaluation of grasp capability of a gripper driven by optimal spherical mechanism,” *Mech. Mach. Theory* **166**, 104486 (2021).
- [30] S. Krut, V. Bégoc, E. Dombre and F. Pierrot, “Extension of the form-closure property to underactuated hands,” *IEEE Trans. Robot.* **26**(5), 853–866 (2010).